

Research



**Cite this article:** Sarkar B, Maiti S, Jadhav GR, Paira P. 2018 Discovery of benzothiazolylquinoline conjugates as novel human A<sub>3</sub> receptor antagonists: biological evaluations and molecular docking studies.

*R. Soc. open sci.* **5**: 171622.

<http://dx.doi.org/10.1098/rsos.171622>

Received: 14 October 2017

Accepted: 8 January 2018

**Subject Category:**

Chemistry

**Subject Areas:**

medicinal chemistry/computational chemistry/organic chemistry

**Keywords:**

benzothiazolylquinoline, human A<sub>3</sub> receptor antagonist, molecular docking, radioligand binding assay, glide score

**Authors for correspondence:**

Priyankar Paira

e-mail: [priyankar.paira@vit.ac.in](mailto:priyankar.paira@vit.ac.in)

<sup>†</sup>These authors contributed equally to the study.

This article has been edited by the Royal Society of Chemistry, including the commissioning, peer review process and editorial aspects up to the point of acceptance.

Electronic supplementary material is available online at <https://doi.org/10.6084/m9.figshare.c.3983964>.



# Discovery of benzothiazolylquinoline conjugates as novel human A<sub>3</sub> receptor antagonists: biological evaluations and molecular docking studies

Bidisha Sarkar<sup>†</sup>, Santanu Maiti<sup>†</sup>, Gajanan Raosaheb Jadhav and Priyankar Paira

Department of Chemistry, School of Advanced Sciences, VIT University, Vellore, Tamil Nadu 632014, India

PP, 0000-0003-1698-4895

Adenosine is known as an endogenous purine nucleoside and it modulates a wide variety of physiological responses by interacting with adenosine receptors. Among the four adenosine receptor subtypes, the A<sub>3</sub> receptor is of major interest in this study as it is overexpressed in some cancer cell lines. Herein, we have highlighted the strategy of designing the hA<sub>3</sub> receptor targeted novel benzothiazolylquinoline scaffolds. The radioligand binding data of the reported compounds are rationalized with the molecular docking results. Compound **6a** showed best potency and selectivity at hA<sub>3</sub> among other adenosine receptors.

## 1. Introduction

Adenosine is an endogenous purine nucleoside which regulates many physiological functions through the activation of four specific receptor subtypes, classified as A<sub>1</sub>, A<sub>2A</sub>, A<sub>2B</sub> and A<sub>3</sub> adenosine receptors (AR), belonging to the family of G-protein-coupled receptors [1]. These receptors are widely distributed in mammalian tissues. The A<sub>3</sub>AR subtype is the most recently characterized member of the family which was first cloned from a rat testis cDNA library [2] and is still undergoing intensive pharmacological characterization. The A<sub>3</sub>AR subtype is implicated in various pathological conditions such as cardiac and cerebral ischaemia, neurodegenerative diseases as well as inflammatory pathologies including rheumatoid arthritis and asthma [3]. Furthermore, A<sub>3</sub>AR is overexpressed in various

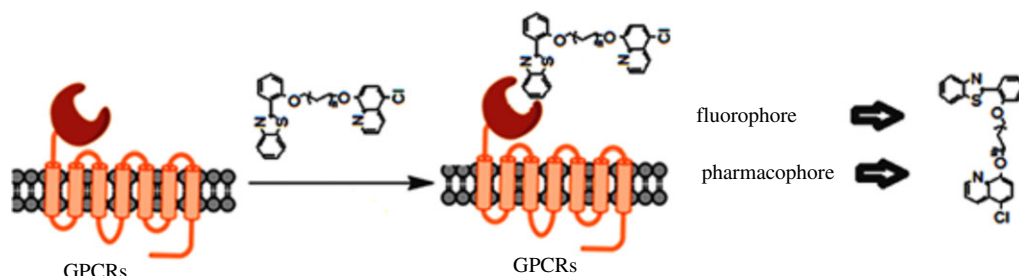


**Figure 1.** Dual role: pharmacophore as well as a fluorophore. G-PCR, G-protein coupled receptor.

neoplastic cells including HL-60 leukaemia, human Jurkat T-cell lymphoma, astrocytoma, A378 melanoma, B16-F10 and solid tumour (e.g. a two–threefold increase in colon carcinomas), while low or almost no receptor expression was found in normal cells [4,5].

Similar results were found in studies of the receptor expression levels in tumour tissues derived from patients with colon, breast, small cell lung, pancreatic and hepatocellular carcinomas and melanoma in direct comparison with adjacent body normal tissues [6–15]. Higher  $A_3AR$  expression in the tumour versus adjacent non-neoplastic tissue was further confirmed by reverse transcription-PCR analysis of colon and breast carcinoma. Protein analysis of  $A_3AR$  expression in fresh tumours derived from colon ( $n = 40$ ) or breast ( $n = 17$ ) revealed 61% and 78% higher expression in the tumour than adjacent normal tissue, respectively [16]. Thus the  $A_3$  receptor could be a prospective therapeutic target and biological predictive marker in cancer therapy. The high  $A_3AR$  expression level in the tumour tissues was associated with elevated nuclear factor  $\kappa B$  and cyclin D1 levels [16]. High  $A_3AR$  mRNA expression was also exhibited in other solid tumour types. Mechanistic studies demonstrated that  $A_3AR$  activation by synthetic agonists or antagonists induces down-regulation of key cell growth-regulatory proteins including cyclin D1 and nuclear factor  $\kappa B$  [10,17,18]. Hence, discovery of selective  $A_3AR$  targeting ligands has been a great challenge in last two decades. Moreover,  $A_3AR$  antagonists research not only aids in the development of therapeutic agents but also in the development of diagnostic agents [2,19]. Nowadays, the diagnostic approaches have been significantly developed by using fluorescently labelled pharmacophores.

In the past few years, there have been strenuous efforts to develop different heterocyclic scaffolds as  $hA_3$  antagonists including pyridine and dihydropyridine analogues, flavonoid, isoquinoline, triazoloquinazolines, pyrazolo-[3,4-*c*]or-[4,3-*c*]quinolones, triazoloquinoxaline, pyrazolo-[4,3-*e*]1,2,4-triazolo-[1,5-*c*]pyrimidines, ruthenium-pyrazolopyrimidines [20–29]. However, none of the pharmacophores has been tested in  $A_3$  overexpressed cancer cell lines. The cellular imaging study and cell surface receptor localization study was also not performed because these scaffolds are nonfluorescent. Therefore, to identify the  $hA_3$  targeting novel fluorescent ligands, a molecular simplification followed by molecular docking approach was employed.

Benzothiazole possesses several biological activities such as anti-inflammatory, antimicrobial, anti-HIV, anticancer and amyloid marker [30–36]. These scaffolds are also able to arrest metal promoted amyloid fibril build-up [37]. Likewise, 8-hydroxy quinoline has also been developed as potent bioactive scaffold [38]. Herein, we have highlighted the strategy of designing the novel 2-(2'-hydroxyphenyl)benzothiazole (HBT) scaffolds having dual properties (pharmacophore and fluorophore) via molecular simplification followed by a molecular docking approach (figure 1). The designed molecules have already shown potency and selectivity in  $hA_3AR$  overexpressed cancer cell lines than normal cell lines [38]. In our earlier report, the cellular localization was also observed using those scaffolds. To justify the molecular pathway of these drugs, we have initiated the molecular docking approach as well as radioligand binding study at  $hA_3AR$ .

## 2. Results and discussion

### 2.1. Chemistry

#### 2.1.1. Molecular simplification

Following a molecular simplification approach, we have identified the benzothiazolyquinoline ring system as an appropriate core skeleton for the design of novel fluorescent  $hA_3AR$  antagonists. Here,

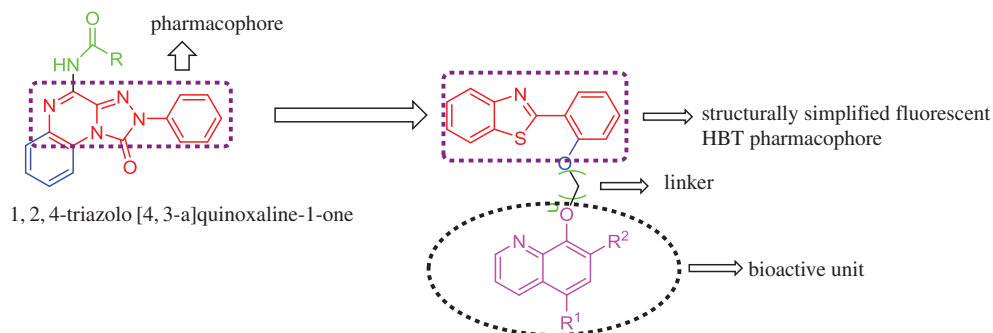
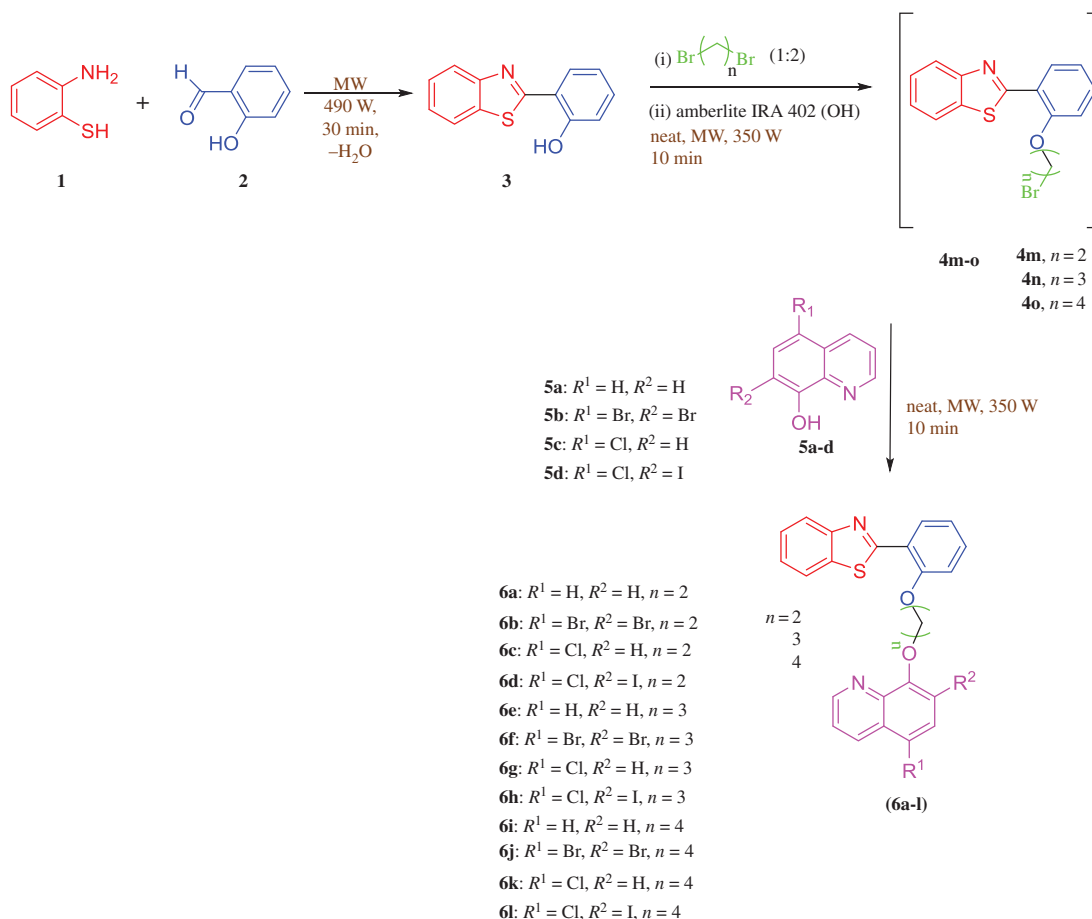


**Figure 2.** Molecular simplification approach to design the  $hA_3$  targeting ligand.



**Scheme 1.** Preparation of 8-[2-(2-benzothiazol-2-yl-phenoxy)-alkoxy]-quinoline derivatives (6a-l) [38].

we have simplified the structure of the tricyclic  $A_3$  antagonist (triazoloquinoxaline) into bicyclic motif (2-benzothiazolyl phenol). In the course of structure design, we have attached the bicyclic fluorescent pharmacophore (2-benzothiazolyl phenol) with another bioactive 8-hydroxy quinolone unit through a linker to enhance the  $A_3$  binding ability (figure 2).

## 2.2. Synthesis

In our earlier report, a series of 2-(2'-hydroxyphenyl)benzothiazolylquinoline scaffolds were prepared in conventional way and also under microwave condition in one pot sequence (scheme 1) [38]. We followed the earlier reported green method to synthesize the following scaffolds and then characterized

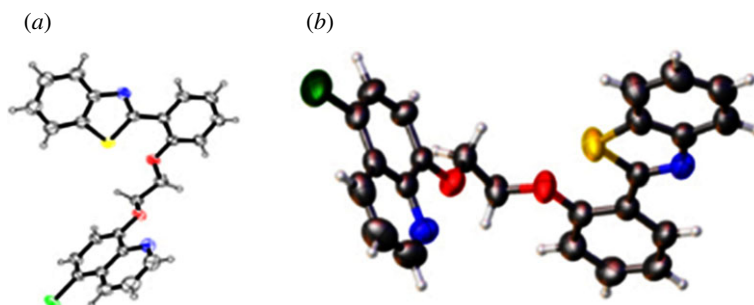


**Figure 3.** ORTEP diagrams of compound **6c** drawn at the 50% probability level [38].

**Table 1.** Binding energy of benzothiazolylquinoline analogues (**6a–l**) with  $hA_3$ .

entry	compound	GLIDE score (Kcal mol <sup>−1</sup> )
1	<b>6a</b>	−10.31
2	<b>6b</b>	−9.06
3	<b>6c</b>	−6.50
4	<b>6d</b>	−8.90
5	<b>6e</b>	−9.05
6	<b>6f</b>	−8.81
7	<b>6g</b>	−9.04
8	<b>6h</b>	−8.78
9	<b>6i</b>	−7.48
10	<b>6j</b>	−8.37
11	<b>6k</b>	−9.05
12	<b>6l</b>	−9.36

by <sup>1</sup>H NMR, <sup>13</sup>C NMR and LCMS study (electronic supplementary material, supporting information). Structure of compound **6c** was further confirmed by single crystal X-ray study (figure 3) [38].

## 2.3. Molecular docking studies

### 2.3.1. Homology modelling

The crystallographic structure of  $hA_{2A}$ AR complexed with ZM-241385 as a high affinity antagonist (PDB code: 3EML) [39]. It was already being used to build up a homology model of the  $hA_3$ AR by our group [40]. Considering the high resolution (2.6 Å) and accuracy of the structure of  $hA_{2A}$ AR, 3EML was selected as a template by various research groups [41,42]. MODELLER 9.11 was used to perform the homology modelling [43–46] and the quality of the model was evaluated using the Ramachandran plot. Subsequently, the prediction ability of the constructed  $hA_3$ AR homology model was evaluated in the molecular docking experiments using the GLIDE tool from Schrödinger maestro.

### 2.3.2. Molecular docking

Our approach was to select a new class of  $hA_3$ AR targeting compounds from a group of hypothetically designed 2-phenylbenzothiazole (HBT)-based scaffolds. We performed molecular docking of 12 different HBT-based ligands using the GLIDE tool from Schrödinger maestro to identify the hypothetical binding mode at the  $hA_3$ AR. Finally, we have identified the best inhibitor for targeted  $hA_3$ AR from GLIDE scores (table 1).

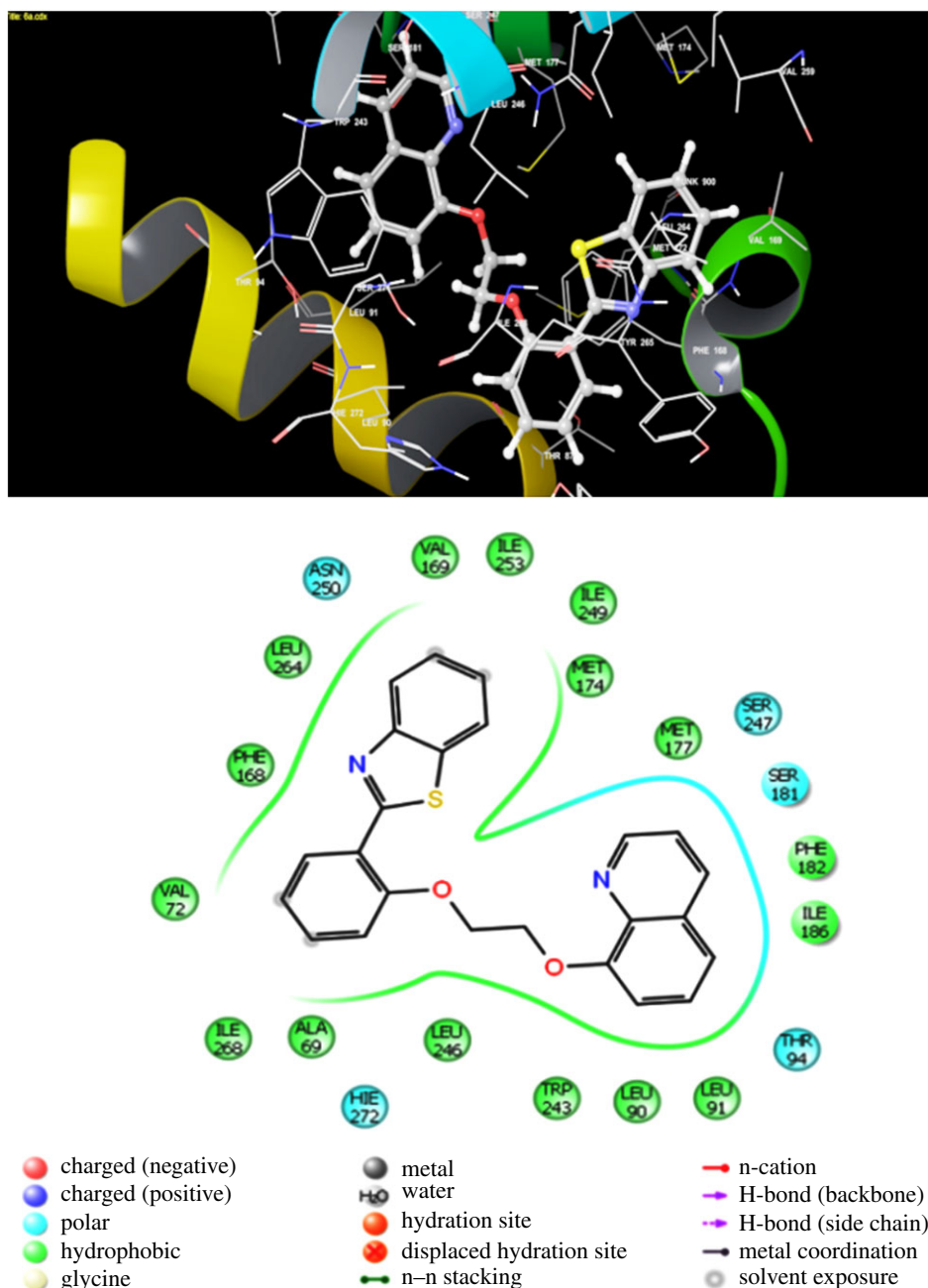


**Figure 4.** Binding interaction of most potent benzothiazolylquinoline analogue (**6a**) with  $hA_3$  receptor.

All the newly synthesized benzothiazolylquinoline scaffolds were docked into the orthosteric transmembrane-binding cavities of  $hA_3$ AR. From the ligand docking, we have inferred that out of 12 synthesized scaffolds, compound **6a** displayed the best GLIDE score with the lowest binding energy. In figure 4, the hypothetical binding pose of compound **6a** is clearly observed at the  $hA_3$ AR. In particular, the most prominent aromatic  $\pi$ - $\pi$  stacking interactions are established between Phe 168 and ligands and it was anchored properly within the binding cleft. Moreover, a strong hydrogen bond with Phe 168 was also appeared within the binding pocket. Likewise, a strong  $\pi$ - $\pi$  stacking interaction was observed between Tyr 265 and compound **6f**. Compound **6g** also formed a hydrogen bond with Val 169 (electronic supplementary material, figure S1)

### 2.3.3. Binding affinity at $hA_1$ AR, $hA_{2A}$ AR, $hA_{2B}$ AR and $hA_3$ AR

The receptor binding affinities of the synthesized benzothiazolylquinoline derivatives (**6a-l**) are recapitulated in table 2. The binding affinity of the antagonist was estimated by measuring the

**Table 2.** Binding affinity ( $K_i$ ) of synthesized compounds at  $hA_1$ AR,  $hA_{2A}$ AR and  $hA_3$ AR and selectivity against  $hA_1$ AR and  $hA_{2A}$ AR.

compound	$K_i$ , $\mu$ M (95% CI) <sup>d</sup>				selectivity	
	$hA_1$ <sup>b</sup>	$hA_{2A}$ <sup>c</sup>	$hA_{2B}$ <sup>a</sup>	$hA_3$ <sup>e</sup>	$hA_1/A_3$ $hA_{2A}/A_3$	
<b>6a</b>	>100	23.8 (21.6–26.4)	>30	2.6 (1.8–4.5)	>38.46	>11.53
<b>6b</b>	>100	17.2 (15.3–19.4)	>20	3.2 (2.4–4.1)	>31.25	>6.25
<b>6c</b>	30.8 (26.5–32.7)	32.8 (28.7–34.1)	>20	30.4 (27.6–32.1)	1.01	>19.80
<b>6d</b>	>100	>20	>20	5.6 (3.8–7.1)	>17.85	>3.57
<b>6e</b>	>100	>20	>30	3.8 (2.6–4.7)	>26.31	>7.89
<b>6f</b>	>100	>20	>30	6.2 (4.8–7.1)	>16.12	>4.83
<b>6g</b>	>100	>20	>20	4.2 (3.1–5.4)	>23.80	>4.76
<b>6h</b>	>100	>20	>20	6.1 (4.9–7.2)	>16.39	>3.27
<b>6i</b>	29.7 (27.8–32.6)	34.9 (32.7–37.1)	>20	25.4 (23.6–27.1)	1.16	>0.78
<b>6j</b>	>100	>20	>20	6.4 (4.9–8.2)	>15.62	>3.15
<b>6k</b>	>100	>20	>10	3.7 (2.7–4.8)	>27.02	>2.70
<b>6l</b>	>100	>20	>30	3.6 (2.1–4.8)	>27.77	>8.33

<sup>a</sup>Adenylyl cyclase activity of synthesized compounds at the  $hA_{2B}$ AR.

<sup>b</sup>Displacement of specific [3H]-CCPA binding at  $hA_1$ AR expressed in Chinese hamster ovary (CHO) cells ( $n = 3-6$ ).

<sup>c</sup>Displacement of specific [3H]-5'-*N*-ethylcarboxamido adenosine (NECA) binding at  $hA_{2A}$ AR expressed in CHO cells ( $n = 3-6$ ).

<sup>d</sup> $K_i$  values for inhibition of NECA-stimulated adenylyl cyclase activity in CHO cells ( $n = 3-6$ ).

<sup>e</sup>Displacement of specific [3H]-2-(1-hexynyl)-*N*<sup>6</sup>-methyl adenosine (HEMADO) binding at  $hA_3$ AR expressed in CHO cells ( $n = 3-6$ ).

displacement of selective radioligands which were formerly bound to the receptor expressed (Chinese hamster ovary cells (CHO) for  $hA_1$ AR,  $hA_{2A}$ AR and  $hA_3$ AR) at the surface of the cell. In this particular assay, the displacement of: (i) specific [3H] CCPA (2-chloro-*N*(6)-cyclopentyladenosine) binding at  $hA_1$ AR, (ii) specific [3H] NECA (5'-*N*-ethylcarboxamido adenosine) binding at the  $hA_{2A}$ AR, and (iii) [3H] HEMADO (2-(1-hexynyl)-*N*<sup>6</sup>-methyladenosine) at the  $hA_3$ AR were evaluated. There is no suitable radioligand for  $hA_{2B}$ AR found and hence the antagonists activity was determined in adenylyl cyclase experiments in CHO cells expressing the  $hA_{2B}$ AR [47,48].  $K_i$  (dissociation constant) value of the data was calculated using the Cheng and Prusoff equation [49], with geometric means of at least three experiments including 95% confidence intervals. From table 2, it was observed that most of the compounds exhibited a  $K_i$  value at  $hA_3$  in the range of 2–6  $\mu$ M. Compound **6c** and **6i** showed least binding efficacy with  $hA_3$  which is clearly rationalized with their binding energy profile (GLIDE score). Compound **6a** exhibited the most binding potency at  $hA_3$  in the 2.6  $\mu$ M range. This compound has also shown 38-fold and 11-fold more selective potency at  $hA_3$  than  $hA_1$  and  $hA_{2A}$ , respectively. While increasing the length of the  $-CH_2-$  linker from 2 to 3, binding potency of the compound **6e** at  $hA_3$  is reduced to 3.8  $\mu$ M. Selectivity of this compound at  $hA_3$  with respect to  $hA_1$  and  $hA_2$  has also been reduced to some extent. Consequently, compound **6i** showed much less potency and selectivity in  $hA_3$ . Compounds (**6f-h** and **6j-l**) having electronegative groups and lengthy linkers ( $n = 3, 4$ ) showed good potency and selectivity at  $hA_3$ . It was also observed that compound **6b** having two electronegative bromine groups with a small linker ( $n = 2$ ) exhibited good potency (3.2  $\mu$ M) and selectivity at  $hA_3$ .

### 3. Experimental

#### 3.1. Biology

##### 3.1.1. Chinese hamster ovary membranes preparation

The human  $A_1$ ,  $A_{2A}$ ,  $A_{2B}$ , and  $A_3$ ARs were transfected in CHO cells based on the previously reported method [47–50]. The cells were grown adherently and maintained in Dulbecco's modified Eagle's medium with nutrient mixture F12 (DMEM/F12) without nucleosides, containing 10% foetal calf serum, streptomycin (100  $\mu$ g ml<sup>-1</sup>), penicillin (100  $\mu$ g ml<sup>-1</sup>), L-glutamine (2 mM) and Geneticin (G418, 0.2 mg ml<sup>-1</sup>) at 37°C in 5% CO<sub>2</sub>, 95% air. The membrane preparation was initiated by removal of



culture medium followed by washing of the cells with phosphate buffered saline and scraped off T75 flasks in ice-cold hypotonic buffer (5 mM Tris-HCl, 2 mM EDTA, pH 7.4). Then the cell suspension was homogenized with a polytron, and the homogenate was centrifuged for 10 min at 1000 g. The supernatant was then centrifuged for 30 min at 100 000 g. The membrane pellet was suspended in (i) 50 mM Tris-HCl buffer, pH 7.4, for A<sub>1</sub> ARs; (ii) 50 mM Tris-HCl, 10 mM MgCl<sub>2</sub> buffer, pH 7.4, for A<sub>2A</sub> ARs; and (iii) 50 mM Tris-HCl, 10 mM MgCl<sub>2</sub>, 1 mM EDTA buffer, pH 7.4, for A<sub>3</sub> ARs. The cell suspension was incubated with adenosine deaminase for 30 min at 37°C. Then the membrane preparation was used for binding experiments.

### 3.1.2. Binding at human A<sub>1</sub>, A<sub>2A</sub> and A<sub>3</sub> adenosine receptors

For radioligand binding at A<sub>1</sub> ARs 1 nM [3H] CCPA was used, whereas 30 nM of [3H] NECA were used for A<sub>2A</sub> and 10 nM of [3H]- HEMADO were used for A<sub>3</sub> receptors, respectively [47–50]. Nonspecific binding of [3H]CCPA was determined in the presence of 1 mM theophylline, when [3H]NECA 100 µM R-PIA was used.

### 3.1.3. Adenylyl cyclase activity

The potency of antagonists at the A<sub>2B</sub> AR was determined in adenylyl cyclase experiments [47–50]. For the measurement of adenylyl cyclase activity, only one high speed centrifugation of the homogenate was used. The resulting crude membrane pellet was resuspended in 50 mM Tris-HCl, pH 7.4 and immediately used for the cyclase assay.

### 3.1.4. Data analysis

Inhibitory binding constants,  $K_i$ , were calculated from the IC<sub>50</sub> values according to the Cheng and Prusoff equation  $K_i = IC_{50} / (1 + [C^*] / KD^*)$ , where [C\*] is the concentration of the radioligand and KD\* its dissociation constant [49,50]. A weighted nonlinear least-squares curve fitting program LIGAND was also used for computer analysis of inhibition experiments. Potency values (IC<sub>50</sub>) obtained in cyclic AMP assays were calculated by nonlinear regression analysis using the equation for a sigmoid concentration–response curve (Graph Pad Prism, San Diego, CA, USA). All experimental data are expressed as geometric mean with 95% confidence limits in parentheses of three or four independent experiments performed in duplicate.

## 4. Conclusion

In summary, we have designed a class of benzothiazolylquinoline scaffolds for the hA<sub>3</sub> target. Molecular simplification and molecular docking approach using the GLIDE tool from Schrödinger maestro has been employed for the design of these drugs. The effective binding modes of the scaffolds with the receptor binding sites were clearly explained. In addition, we have also performed radioligand binding assay of these scaffolds at hA<sub>1</sub> AR, hA<sub>2A</sub> AR, hA<sub>2B</sub> AR and hA<sub>3</sub> AR. We observed that compound **6a** exhibited maximum potency and selectivity in hA<sub>3</sub> AR with respect to hA<sub>1</sub> AR, hA<sub>2A</sub> AR and hA<sub>2B</sub> AR which is rationalized with a docking study. Finally, it was concluded that these cytotoxic molecules are selectively targeting to the hA<sub>3</sub> AR.

**Ethics.** The department was ethically approved by UGC.

**Data accessibility.** Molecular docking images of selected compounds can be found in the electronic supplementary material.

**Authors' contributions.** B.S. and S.M. synthesized and characterized the compounds. B.S. has performed the molecular docking study. B.S. and S.M. contributed equally in this paper. G.R.J. did the radioligand binding assay for this paper. B.S., S.M. and G.R.J. drafted the manuscript. All the authors analysed and discussed the results and revised the manuscript.

**Competing interests.** We have no competing interests.

**Funding.** The authors are grateful to VIT University for seed funding. We acknowledge DST, New Delhi, India for the DST-FIST project. We also acknowledge DST-SERB, India for a young scientist grant and the DST-SERB EMR project for providing us with funding.

**Acknowledgements.** The authors thank VIT University for providing us with laboratory facilities.

- Haskó G, Linden J, Cronstein B, Pacher P. 2008 Adenosine receptors: therapeutic aspects for inflammatory and immune diseases. *Nat. Rev. Drug Discov.* **7**, 759–770. (doi:10.1038/nrd2638)
- Baraldi PG, Preti D, Borea PA, Varani K. 2012 Medicinal chemistry of A<sub>3</sub> adenosine receptor modulators: pharmacological activities and therapeutic implications. *J. Med. Chem.* **55**, 5676–5703. (doi:10.1021/jm300087j)
- Moro S, Gao ZG, Jacobson KA, Spalluto G. 2006 Progress in the pursuit of therapeutic adenosine receptor antagonists. *Med. Res. Rev.* **26**, 131–159. (doi:10.1002/med.20048)
- Gessi S, Varani K, Merighi S, Cattabriga E, Iannotta V, Leung E, Baraldi PG, Borea PA. 2002 A3 adenosine receptors in human neutrophils and promyelocytic HL60 cells: a pharmacological and biochemical study. *Mol. Pharmacol.* **61**, 415–424. (doi:10.1124/mol.61.2.415)
- Gessi S *et al.* 2004 Elevated expression of A3 adenosine receptors in human colorectal cancer is reflected in peripheral blood cells. *Clin. Cancer Res.* **10**, 5895–5901. (doi:10.1158/1078-0432.CCR-1134-03)
- Fishmana P, Bar-Yehudaa S, Liang BT, Jacobsonc KA. 2012 Pharmacological and therapeutic effects of A3 adenosine receptor agonists. *Drug Discov. Today* **17**, 359–366. (doi:10.1016/j.drudis.2011.10.007)
- Ohana G, Bar-Yehuda S, Arich A, Madi L, Drenick Z, Rath-Wolfson L, Silberman D, Slosman G, Fishman P. 2003 Inhibition of primary colon carcinoma growth and liver metastasis by the A3 adenosine receptor agonist CF101. *Br. J. Cancer* **89**, 1552–1558. (doi:10.1038/sj.bjc.6601315)
- Kamiya H, Kanno T, Fujita Y, Gotoh A, Nakano T, Nishizaki T. 2012 Apoptosis-related gene transcription in human A549 lung cancer cells via A3 adenosine receptor. *Cell Physiol. Biochem.* **29**, 687–696. (doi:10.1159/000312589)
- Fishman P, Bar-Yehuda S, Rath-Wolfson L, Barrer F, Rath-Ochaion A, Madi L. 2003. Targeting the A3 adenosine receptor for cancer therapy: inhibition of prostate carcinoma cell growth by A3AR agonist. *Anticancer Res.* **23**, 2077–2083.
- Madi L, Bar-Yehuda S, Barrer F, Ardon E, Ochaion A, Fishman P. 2003 A3 adenosine receptor activation in melanoma cells. *J. Biol. Chem.* **278**, 42 121–42 130. (doi:10.1074/jbc.M301243200)
- Gessi S, Varani K, Merighi S, Morelli A, Ferrari D, Leung E, Baraldi PG, Spalluto G, Borea PA. 2001 Pharmacological and biochemical characterization of A3 adenosine receptors in Jurkat T cells. *Br. J. Pharmacol.* **134**, 116–126. (doi:10.1038/sj.bjp.0704254)
- Merighi S, Varani K, Gessi S, Cattabriga E, Iannotta V, Ulouglu C, Leung E, Borea PA. 2001 Pharmacological and biochemical characterization of adenosine receptors in the human malignant melanoma A375 cell line. *Br. J. Pharmacol.* **134**, 1215–1226. (doi:10.1038/sj.bjp.0704352)
- Suh BC, Kim TD, Lee JU, Seong JK, Kim KT. 2001 Pharmacological characterization of adenosine receptors in PGT-β mouse pineal gland tumour cells. *Br. J. Pharmacol.* **134**, 132–142. (doi:10.1038/sj.bjp.0704218)
- Trincavelli ML, Tuscano D, Marroni M. 2002 A3 adenosine receptors in human astrocytoma cells: agonist-mediated desensitization, internalization, and down-regulation. *Mol. Pharmacol.* **62**, 1373–1384. (doi:10.1124/mol.62.6.1373)
- Auchampach JA, Xiaowei J, Tina CW, George H, Caughey GH, Linden J. 1997 Canine mast cell adenosine receptors: cloning and expression of the A3 receptor and evidence that degranulation is mediated by the A2B receptor. *Mol. Pharmacol.* **52**, 846–860. (doi:10.1124/mol.52.5.846)
- Madi L *et al.* 2004 The A3 adenosine receptor is highly expressed in tumor versus normal cells: potential target for tumor growth inhibition. *Clin. Cancer Res.* **10**, 4472–4479. (doi:10.1158/1078-0432.CCR-03-0651)
- Fishman P, Madi L, Bar-Yehuda S, Barrer F, Del Valle L, Khalili K. 2002 Evidence for involvement of Wnt signaling pathway in IB-MECA mediated suppression of melanoma cells. *Oncogene* **21**, 4060–4064. (doi:10.1038/sj.onc.1205531)
- Fishman P, Bar-Yehuda S, Barrer F, Madi L, Multani AF, Pathak S. 2001 The A3 adenosine receptor as a new target for cancer therapy and chemoprotection. *Exp. Cell Res.* **269**, 230–236. (doi:10.1006/excr.2001.5327)
- Catarzi D *et al.* 2015 1,2,4-Triazolo[1,5-a]quinoxaline derivatives and their simplified analogues as adenosine A3 receptor antagonists. Synthesis, structure–affinity relationships and molecular modeling studies. *Bioorg. Med. Chem.* **23**, 9–21. (doi:10.1016/j.bmc.2014.11.033)
- Tuccinardi T *et al.* 2008 Substituted Pyrazolo[3,4-b]pyridines as potent A1 adenosine antagonists: synthesis, biological evaluation, and development of an A1 bovine receptor model. *Chem. Med. Chem.* **3**, 898–913. (doi:10.1002/cmdc.2007 00355)
- Press NJ *et al.* 2004 New highly potent and selective adenosine A3 receptor antagonists. *Curr. Top. Med. Chem.* **4**, 863–870. (doi:10.2174/1568026043451023)
- Poli D, Catarzi D, Colotta V, Varano F, Filacchioni G, Daniele S, Moro S. 2011 The identification of the 2-phenylphthalazin-1(2H)-one scaffold as a new decorable core skeleton for the design of potent and selective human A3 adenosine receptor antagonists. *J. Med. Chem.* **54**, 2102–2113. (doi:10.1021/jm101328n)
- Colotta V, Lenzi O, Catarzi D, Varano F, Filacchioni G, Martini C, Moro S. 2009 Pyrido[2,3-e]-1,2,4-triazolo [4,3-a]pyrazin-1-one as a new scaffold to develop potent and selective human A3 adenosine receptor antagonists. Synthesis, pharmacological evaluation, and ligand–receptor modeling studies. *J. Med. Chem.* **52**, 2407–2419. (doi:10.1021/jm8014876)
- Vazquez-Rodriguez S, Matos MJ, Santana L, Uriarte E, Borges F, Kachler S, Klotz K-N. 2013 Chalcone-based derivatives as new scaffolds for h A3 adenosine receptor antagonists. *J. Pharm. Pharmacol.* **65**, 697–703. (doi:10.1111/jphp.12028)
- Tafi A *et al.* 2006 Pharmacophore based receptor modeling: the case of adenosine A3 receptor antagonists. An approach to the optimization of protein models. *J. Med. Chem.* **49**, 4085–4097. (doi:10.1021/jm051112+)
- Settimo FD *et al.* 2007 5-Amino-2-phenyl[1,2,3] triazolo[1,2-a][1,2,4]benzotriazin-1-one: a versatile scaffold to obtain potent and selective A3 adenosine receptor antagonists. *J. Med. Chem.* **50**, 5676–5684. (doi:10.1021/jm0708376)
- Morizzo E *et al.* 2007 Scouting human A3 adenosine receptor antagonist binding mode using a molecular simplification approach: from triazoloquinoxaline to a pyrimidine skeleton as a key study. *J. Med. Chem.* **50**, 6596–6606. (doi:10.1021/jm070852a)
- Kenneth AJ, Athena MK, Dilip KT, Andei AI, Delia P, Pier GB. 2009 Handbook of experimental pharmacology. *Handbook Exp. Pharmacol.* **193**, 123–159. (doi:10.1007/978-3-540-89615-9\_5)
- Paira P, Chow MJ, Venkatesan G, Kosaraju VK, Cheong SL, Klotz K-N, Ang WH, Pastorin G. 2013 Organoruthenium antagonists of human A3 adenosine receptors. *Chem. Eur. J.* **19**, 8321–8330. (doi:10.1002/chem.201203291)
- Bandyopadhyay P, Sathe M, Pomariappan S, Sharma A, Sharma P, Srivastava AK, Kaushik MP. 2011 Exploration of *in vitro* time point quantitative evaluation of newly synthesized benzimidazole and benzothiazole derivatives as potential antibacterial agents. *Bioorg. Med. Chem. Lett.* **21**, 7306–7309. (doi:10.1016/j.bmcl.2011.10.034)
- Solomon VR, Hua C, Lee H. 2009 Hybrid pharmacophore design and synthesis of isatin–benzothiazole analogs for their anti-breast cancer activity. *Bioorg. Med. Chem.* **17**, 7585–7592. (doi:10.1016/j.bmc.2009.08.068)
- Singh MK, Tilak R, Nath G, Awasthi SK, Agarwal A. 2013 Design, synthesis and antimicrobial activity of novel benzothiazole analogs. *Eur. J. Med. Chem.* **63**, 635–644. (doi:10.1016/j.ejmech.2013.02.027)
- Hutchinson I, Bradshaw TD, Matthews CS, Stevens MFG, Westwell AD. 2003 Antitumour benzothiazoles. Part 20: 3'-cyano and 3'-alkynyl-substituted 2-(4'-aminophenyl) benzothiazoles as new potent and selective analogues. *Bioorg. Med. Chem. Lett.* **13**, 471–474. (doi:10.1016/S0960-894X(02)00930-7)
- Chhabra M, Sinha S, Banerjee S, Paira P. 2016 An efficient green synthesis of 2-arylbenzothiazole analogues as potent antibacterial and anticancer agents. *Bioorganic Med. Chem. Lett.* **26**, 213–217. (doi:10.1016/j.bmcl.2015.10.087)
- Christina CC, Caitlin B, Joanna SO, Stephen D, Jerry Y. 2012 Oligovalent amyloid-binding agents reduce sevi-mediated enhancement of HIV-1 infection. *J. Am. Chem. Soc.* **134**, 905–908. (doi:10.1021/ja210931b)
- Rodriguez-Rodriguez C *et al.* 2009 Design, selection, and characterization of thioflavin-based intercalation compounds with metal chelating properties for application in Alzheimer's disease. *J. Am. Chem. Soc.* **131**, 1436–1451. (doi:10.1021/ja806062g)
- Hickey JL *et al.* 2013 Diagnostic imaging agents for Alzheimer's disease: copper radiopharmaceuticals that target Aβ plaques. *J. Am. Chem. Soc.* **135**, 16 120–16 132. (doi:10.1021/ja4057807)
- Chhabra M, Babu LT, Mondal A, Sun H, Paira P. 2017 Amberlite IRA 402(OH) mediated green synthesis of novel benzothiazole–quinoline conjugates as cancer theranostics. *Chemistry Select* **2**, 2480–2486. (doi:10.1002/slct.201700066)



39. Jaakola VP, Griffith MT, Hanson MA, Cherezov V, Chien TEY, Lane JR, Ijzerman AP, Stevens RC. 2008 The 2.6 angstrom crystal structure of a human A2A adenosine receptor bound to an antagonist. *Science* **322**, 1211–1217. (doi:10.1126/science.1164772)
40. Venkatesan G, Paira P, Cheong SL, Vamsikrishna K, Federico S, Klotz K-N, Spalluto G, Pastorin G. 2014 Discovery of simplified N2-substituted pyrazolo[3,4-d]pyrimidine derivatives as novel adenosine receptor antagonists: efficient synthetic approaches, biological evaluations and molecular docking studies. *Bioorg. Med. Chem.* **22**, 1751–1765. (doi:10.1016/j.bmc.2014.01.018)
41. Lenzi O *et al.* 2009 2-Phenylpyrazolo[4,3-d]pyrimidin-7-one as a new scaffold to obtain potent and selective human A<sub>3</sub> adenosine receptor antagonists: new insights into the receptor–antagonist recognition. *J. Med. Chem.* **52**, 7640–7652. (doi:10.1021/jm900718w)
42. Cheong SL *et al.* 2010 The significance of 2-furyl ring substitution with a 2-(*para*-substituted) aryl group in a new series of pyrazolo-triazolo-pyrimidines as potent and highly selective hA<sub>3</sub> adenosine receptors antagonists: new insights into structure–affinity relationship and receptor–antagonist recognition. *J. Med. Chem.* **53**, 3361–3375. (doi:10.1021/jm100049f)
43. Eswar N, Marti-Renom MA, Webb B, Madhusudhan MS, Eramian D, Shen M, Pieper U, Sali A. 2007 Comparative protein structure modeling using Modeller. *Curr. Protoc. Protein Sci.* Wiley **50**, 2.9.1–2.9.31. (doi:10.1002/0471140864.ps0209s50)
44. Marti-Renom MA, Stuart A, Fiser A, Sánchez R, Melo F, Sali A. 2000 Comparative protein structure modeling of genes and genomes. *Annu. Rev. Biophys. Biomol. Struct.* **29**, 291–325. (doi:10.1146/annurev.biophys.29.1.291)
45. Sali A, Blundell TL. 1993 Comparative protein modelling by satisfaction of spatial restraints. *J. Mol. Biol.* **234**, 779–815. (doi:10.1006/jmbi.1993.1626)
46. Fiser A, Do RK, Sali A. 2000 Modeling of loops in protein structures. *Protein Sci.* **9**, 1753–1773. (doi:10.1110/ps.9.9.1753)
47. Klotz KN, Hessling J, Hegler J, Owman C, Kull B, Fredholm BB, Lohse MJ. 1998 Comparative pharmacology of human adenosine receptor subtypes—characterization of stably transfected receptors in CHO cells. *Naunyn-Schmiedeberg's Arch. Pharmacol.* **357**, 1–9. (doi:10.1007/PL00005131)
48. Klotz KN, Cristalli G, Grifantini M, Vittori S, Lohse MJ. 1985 Photoaffinity labeling of A1-adenosine receptors. *J. Biol. Chem.* **260**, 14659–14664.
49. Cheng YC, Prusoff WH. 1973 Relationship between the inhibition constant (KI) and the concentration of inhibitor which causes 50 per cent inhibition (I50) of an enzymatic reaction. *Biochem. Pharmacol.* **22**, 3099–3108. (doi:10.1016/0006-2952(73)90196-2)
50. De Lean A, Hancock AA, Lefkowitz RJ. 1982 Validation and statistical analysis of a computer modeling method for quantitative analysis of radioligand binding data for mixtures of pharmacological receptor subtypes. *Mol. Pharmacol.* **21**, 5–16.